Supplementary Materials

Robust inference for geographic regression discontinuity designs: assessing the impact of police precincts

Emmett B. Kendall, Brenden Beck, Joseph Antonelli

Contents

1 Identification of causal effects

Here we show how the causal effects of interest can be identified from the observed data. First, we examine $\theta(R_\delta)$, which represents the average treatment effect within a distance of δ from the boundary.

$$\begin{aligned}
\theta(R_\delta) &= E[Y^1(R_\delta) - Y^0(R_\delta)] \\
&= E[Y^1(R_{\delta,1}) + Y^1(R_{\delta,0}) \\
&\qquad - Y^0(R_{\delta,1}) - Y^0(R_{\delta,0})] \\
&= E[Y^1(R_{\delta,1}) + Y^1(R_{\delta,1}) \\
&\qquad - Y^0(R_{\delta,0}) - Y^0(R_{\delta,0})] \quad \text{by assumption 2a} \\
&= 2E[Y^1(R_{\delta,1}) - Y^0(R_{\delta,0})] \\
&= 2E[Y(R_{\delta,1}) - Y(R_{\delta,0})] \quad \text{by assumption 1.}
\end{aligned}$$

Next, we examine identification of $\tau(\boldsymbol{b})$ for any location $\boldsymbol{b} \in \mathcal{B}$. Identification of τ follows immediately as it is simply a weighted average of $\tau(\boldsymbol{b})$ for some weight function $w(\boldsymbol{b})$. Note here that we use the notation $\lim_{\boldsymbol{s}\to\boldsymbol{b}^1}$ to denote a limit that approaches the boundary location $\boldsymbol{b}$ from the precinct 1 side of the boundary, with an analogous notation for precinct 0.

$$\begin{aligned}
\tau(\boldsymbol{b}) &= \lambda^1(\boldsymbol{b}) - \lambda^0(\boldsymbol{b}) \\
&= \lim_{\boldsymbol{s}\to\boldsymbol{b}^1} \lambda^1(\boldsymbol{b}) - \lim_{\boldsymbol{s}\to\boldsymbol{b}^0} \lambda^0(\boldsymbol{b}) \quad \text{by assumption 2b} \\
&= \lim_{\boldsymbol{s}\to\boldsymbol{b}^1} \lambda(\boldsymbol{b}) - \lim_{\boldsymbol{s}\to\boldsymbol{b}^0} \lambda(\boldsymbol{b}) \quad \text{by assumption 1.}
\end{aligned}$$

Both of these terms in the final calculation are identifiable from the observed data as we can estimate the observed intensity surface on the two sides of the boundary, separately.

2 Identification and estimation incorporating covariates

In this section, we show how relaxed identification assumptions that incorporate covariates can be used to identify $\tau(\boldsymbol{b})$. Throughout, it is assumed that we observe a vector of covariates at any spatial location $\boldsymbol{s}$, which we refer to as $\boldsymbol{V}(\boldsymbol{s})$. Note that this notation does not necessarily imply that these covariates are spatially correlated in the sense that $\text{cov}(\boldsymbol{V}(\boldsymbol{s}), \boldsymbol{V}(\boldsymbol{s}'))$ is higher when $\boldsymbol{s}$ and $\boldsymbol{s}'$ are closer to each other. It simply implies that the covariates have a distinct value at each location in the spatial domain. In the motivating study, these could represent variables such as socioeconomic status, which varies across the city. For this section, we must also define a spatial point process, which is a function of these covariates. For the observed data, we now have an intensity surface $\lambda(\boldsymbol{s}, \boldsymbol{v})$. This intensity surface is such that

$$E(Y(R)) = \int_{s\in R} \lambda(\boldsymbol{s}, \boldsymbol{V}(\boldsymbol{s}))d\boldsymbol{s},$$

for any region R. We have analogous definitions for the potential intensity surfaces under any particular treatment level $t \in \{0, 1\}$. In the context of $t = 1$, we have $\lambda^1(\boldsymbol{s}, \boldsymbol{v})$, where the intensity surface is such that

$$E(Y^1(R)) = \int_{s\in R} \lambda^1(\boldsymbol{s}, \boldsymbol{V}(\boldsymbol{s}))d\boldsymbol{s}.$$

With these definitions in hand, we can proceed with identification of an analogous estimand to $\tau(\boldsymbol{b})$ that additionally incorporates covariates into the identification assumptions.

Given that our estimand is itself defined in terms of potential intensity functions, which we have now defined to be functions of covariates, we must first adapt our estimand accordingly. Specifically, we focus on an estimand defined by

$$\tau(\boldsymbol{b}, \boldsymbol{V}(\boldsymbol{b})) = \lambda^1(\boldsymbol{b}, \boldsymbol{V}(\boldsymbol{b})) - \lambda^0(\boldsymbol{b}, \boldsymbol{V}(\boldsymbol{b})).$$

We have fixed the covariates at $\boldsymbol{V}(\boldsymbol{b})$, their value at the location of interest. We focus on this as our estimand because it most closely resembles $\tau(\boldsymbol{b})$ from the manuscript as it represents the treatment effect at the boundary of interest. Now

that we have defined our modified estimand, we can also discuss modified identification assumptions that incorporate covariates as follows:

Assumption 2b incorporating covariates: The potential outcome intensity surfaces satisfy

$$\lim_{\boldsymbol{s}\to\boldsymbol{b}} \lambda^t(\boldsymbol{s}, \boldsymbol{V}(\boldsymbol{b})) = \lambda^t(\boldsymbol{b}, \boldsymbol{V}(\boldsymbol{b})) \quad \text{for } t = 0, 1.$$

We can see how this assumption is weaker than Assumption 2b. If there is a discontinuity in the covariates at spatial location $\boldsymbol{b}$, then this will lead to a discontinuity in the potential intensity surface at $\boldsymbol{b}$ as well. This represents a violation in Assumption 2b, and we would incorrectly attribute this discontinuity to being a treatment effect if not addressed. This modified version of Assumption 2b allows there to be discontinuities in the covariates at $\boldsymbol{b}$ as long as the potential intensity surface is continuous with respect to $\boldsymbol{s}$ at $\boldsymbol{b}$ when the covariate values are set to $\boldsymbol{V}(\boldsymbol{b})$, their value at the location of interest. Under this assumption, we can write the estimand of interest as

$$\begin{aligned}
\tau(\boldsymbol{b}, \boldsymbol{V}(\boldsymbol{b})) &= \lambda^1(\boldsymbol{b}, \boldsymbol{V}(\boldsymbol{b})) - \lambda^0(\boldsymbol{b}, \boldsymbol{V}(\boldsymbol{b})) \\
&= \lim_{\boldsymbol{s}\to\boldsymbol{b}^1} \lambda^1(\boldsymbol{s}, \boldsymbol{V}(\boldsymbol{b})) - \lim_{\boldsymbol{s}\to\boldsymbol{b}^0} \lambda^0(\boldsymbol{s}, \boldsymbol{V}(\boldsymbol{b})) \\
&= \lim_{\boldsymbol{s}\to\boldsymbol{b}^1} \lambda(\boldsymbol{s}, \boldsymbol{V}(\boldsymbol{b})) - \lim_{\boldsymbol{s}\to\boldsymbol{b}^0} \lambda(\boldsymbol{s}, \boldsymbol{V}(\boldsymbol{b})).
\end{aligned}$$

This is now a function of the observed data distribution that we can use the observed data to estimate. To estimate $\lim_{\boldsymbol{s}\to\boldsymbol{b}^1} \lambda(\boldsymbol{s}, \boldsymbol{V}(\boldsymbol{b}))$ we can use all data on the precinct 1 side of the boundary to estimate an intensity surface as a function of covariates. Standard software for estimating intensity functions that incorporate covariates available in the `R` package `spatstat` can be used. Additionally, observed data closer to the boundary $\boldsymbol{b}$ should receive more weight in this estimation process, and this is dictated by a spatial smoothness parameter, which can be estimated using cross-validation. While the main identification assumption is weakened somewhat by incorporating covariates, we must make an additional overlap assumption with respect to the covariates of interest. Let $H_1(\boldsymbol{v})$ be the density of $\boldsymbol{V}$ on the precinct 1 side of the boundary, and $H_0(\boldsymbol{v})$ be the density of $\boldsymbol{V}$ on the precinct 0 side of the boundary.

Overlap assumption: Both $H_1(\boldsymbol{V}(\boldsymbol{b})) > 0$ and $H_0(\boldsymbol{V}(\boldsymbol{b})) > 0$.

This assumption states that covariate value $\boldsymbol{V}(\boldsymbol{b})$ must have positive density on both sides of the boundary. This is needed because we need to use data on both sides of the precinct separately to estimate the intensity surface at covariate value $\boldsymbol{V}(\boldsymbol{b})$. Without this assumption, we would be relying entirely on extrapolation to estimate this intensity function.

Overall, these results show that if spatial covariates describing the area of interest are available, then they can be incorporated to weaken the identification assumptions that the GeoRDD design relies upon in the point process setting. We focused on $\tau(\boldsymbol{b})$ throughout, but similar ideas could be used to incorporate covariates when identifying and estimating $\theta(R_\delta)$. One could estimate an intensity surface that is a function of both $\boldsymbol{s}$ and $\boldsymbol{V}(\boldsymbol{s})$ using only data from the precinct 0 side of the boundary, and estimate what is expected to happen on the precinct 1 side of the boundary based on precinct 1's covariate values. A similar process would be done in the reverse order by using data from the precinct 1 side of the boundary to estimate what is expected to happen on the precinct 0 side of the boundary using precinct 0's covariate values. These would provide estimates of $Y^0(R_{\delta,1})$ and $Y^1(R_{\delta,0})$, which could be combined with the observed values for $Y^1(R_{\delta,1})$ and $Y^0(R_{\delta,0})$ in order to provide an estimate of $\theta(R_\delta)$. This requires more extrapolation than for $\tau(\boldsymbol{b})$, however, as the intensity surface model must be extrapolated to a distance of δ from the boundary, as opposed to simply extrapolating to the border itself for $\tau(\boldsymbol{b})$.

3 Theoretical derivations for estimating the null distribution

Here we provide the full mathematical details of the results shown in Section 3.5. First, we can show the type I error rate can be written as:

$$\begin{aligned}
P(\text{reject } H_0 \mid H_0) &= \int_q P(\text{reject } H_0 \mid H_0; \hat{Q}_{1-\alpha} = q) \cdot f_{\hat{Q}}(q) dq \\
&= \int_q P(Z_i > q; X_i) \cdot f_{\hat{Q}}(q) dq \\
&= \int_q [1 - P(Z_i \leq q; X_i)] \cdot f_{\hat{Q}}(q) dq \\
&= 1 - \int_q P(Z_i \leq q; X_i) \cdot f_{\hat{Q}}(q) dq \\
&= 1 - E_{\hat{Q}}[F(X_i, q)].
\end{aligned}$$

This shows that we need $E_{\widehat{Q}}\Big[F(X_i, \widehat{Q}_{1-\alpha})\Big] \geq 1 - \alpha$ in order to obtain type I error control. Next we highlight properties of our estimate of the CDF of the null distribution of the test statistic. First, we can show that the mean of this estimate can be written as:

$$\begin{aligned}
E[\hat{F}(X_i, q)] &= E_{X^{(b)}}\Big[E\Big[\hat{F}(X_i, q)\Big| X_i^{(1)}, X_i^{(2)}, ..., X_i^{(B)}\Big]\Big] \\
&= E_{X^{(b)}}\left[\frac{1}{B}\sum_{b=1}^{B} P(Z_i^{(b)} \leq q; X_i^{(b)})\right] \\
&= E_{X^{(b)}}\left[\frac{1}{B}\sum_{b=1}^{B} F(X_i^{(b)}, q)\right] \\
&= E_{X^{(b)}}\Big[F(X_i^{(b)}, q)\Big] \\
&\approx F(X_i, q) + \frac{d}{dX}F(X_i, q) \cdot E(X_i^{(b)} - X_i) \\
&\quad + \frac{d^2}{dX^2}F(X_i, q) \cdot E\Big[(X_i^{(b)} - X_i)^2\Big]
\end{aligned}$$

This shows that the mean of the CDF estimate depends on how far off the covariates in the null streets, $X_i^{(b)}$, are from the covariates at the precinct boundary of interest, denoted by X_i. Lastly, we can write the variance of our CDF estimate as:

$$\begin{aligned}
Var[\hat{F}(X_i, q)] &= E\Big[Var\Big[\hat{F}(X_i, q)\Big| X^{(b)}\Big]\Big] + Var\Big[E\Big[\hat{F}(X_i, q)\Big| X^{(b)}\Big]\Big] \\
&= E\left[\frac{1}{B^2}\sum_{b=1}^{B} F(X_i^{(b)}, q) \cdot (1 - F(X_i^{(b)}, q))\right] + Var\left[\frac{1}{B}\sum_{b=1}^{B} F(X_i^{(b)}, q)\right] \\
&= \frac{1}{B}E\Big[F(X_i^{(b)}, q) \cdot (1 - F(X_i^{(b)}, q))\Big] + \frac{1}{B}Var[F(X_i^{(b)}, q)] \\
&\approx \frac{1}{B}\left[E\Big[F(X_i^{(b)}, q) \cdot (1 - F(X_i^{(b)}, q))\Big] + Var\left[F(X_i; q) + \frac{d}{dX_i}F(X_i, q)(X_i^{(b)} - X_i)\right]\right] \\
&= \frac{1}{B}\left[E\Big(F(X_i^{(b)}, q) \cdot (1 - F(X_i^{(b)}, q))\Big) + \left(\frac{d}{dX_i}F(X_i, q)\right)^2 \cdot Var(X_i^{(b)})\right]
\end{aligned}$$

For simplicity of exposition, all of these results utilized a scalar covariate X_i, but could be easily extended to accommodate a vector of covariates to match on and analogous results would hold.

4 Investigating covariates used to select null streets

As illustrated in the manuscript, it is important that we sample null streets with similar values of important covariates as the precinct boundaries of interest. This will help to ensure the test statistics at the null streets have a similar distribution as at the precinct borders under the null hypothesis. Figure 1 shows the mean and variance of the test statistics at the null streets after being binned according to the ratio of crime and total crime within a window around a null street (Note: the log of the test statistics are used in this figure to improve visualization in the presence of outlying values). We see that there is a clear relationship between the ratio of crime or total crime and the mean and variance of the test statistic. In particular the variance of the test statistic depends heavily on both of these two variables. This motivates our procedure for finding null streets based on these variables in the NYC policing analysis.

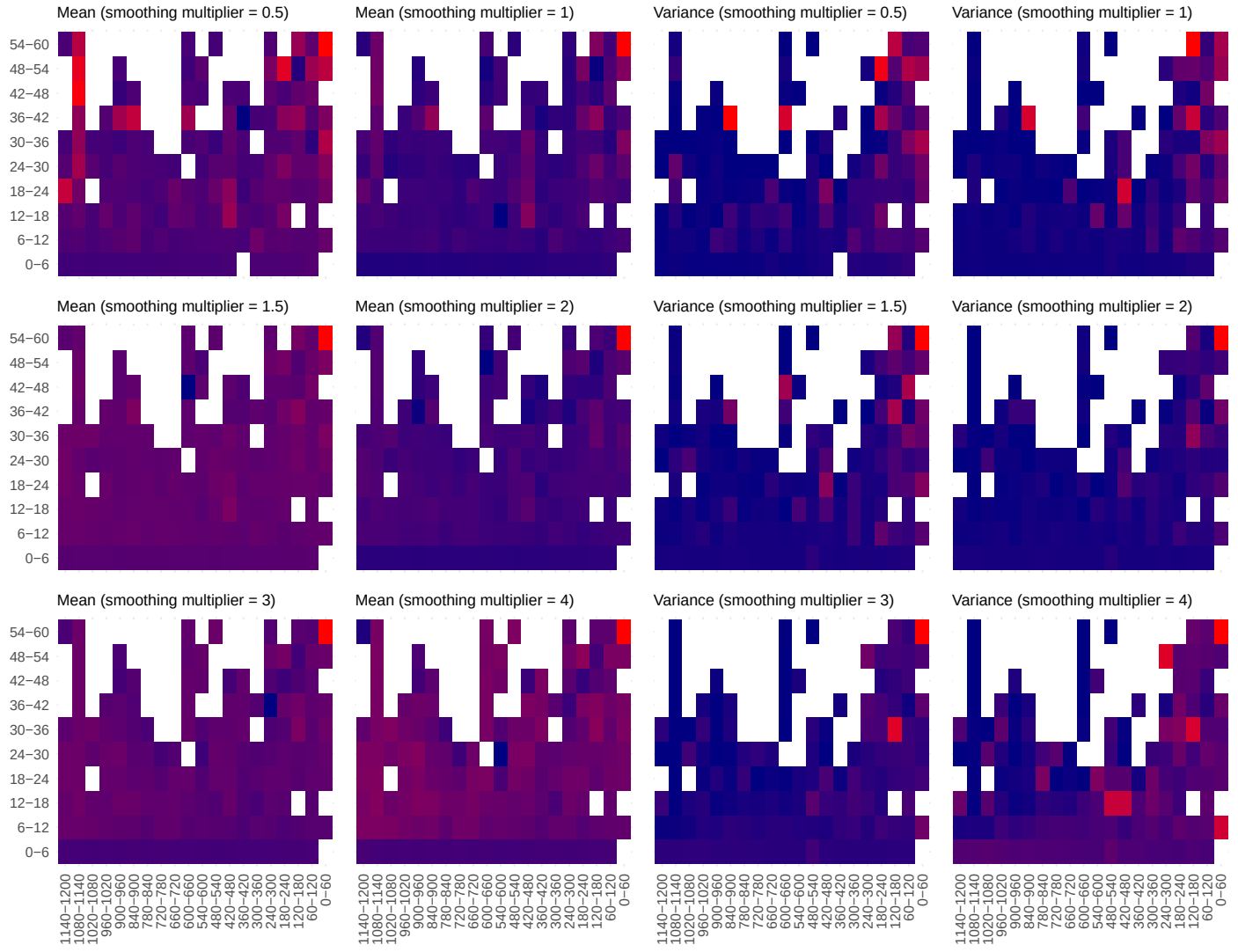

Figure 1: Heat map illustrating the mean (left half) and variance (right half) of the test statistics (on log scale) at the null streets as a function of the ratio of crime (y-axis) and the total amount of crime (x-axis).

5 Additional results using τ as estimand

In this section, we present additional figures and results for the NYC policing analysis and the negative control analysis when using τ as an estimand. First, we show the global test results in the negative control analysis, where we see large p-values regardless of the global test statistic being used or the spatial smoothness level examined. This is expected given that this outcome is a negative control and should not be affected by police precincts. We then provide histograms of p-values from the individual precinct boundary tests across all 144 precincts. We do this for both the negative control analysis and the arrest analysis for a wide range of spatial smoothing parameters. We see that the histograms for the arrest data have slightly more values closer to zero than what one would expect under the null hypothesis of no precinct effect, which highlights the findings in Section 5.3 of the manuscript where more than 5% of the hypothesis tests were rejected. This decreases somewhat as we increase the smoothness of the intensity surface estimates. For the negative control, the histograms appear relatively uniformly distributed, which is again expected given that these outcomes should not be affected by police precincts. These further highlight the ability of our approach to provide valid hypothesis tests in this setting. Lastly, we provide additional results about the choice of c when determining null streets for the negative control analysis. In the manuscript, we showed how results were sensitive to this choice, and that values closer to 1 gave the desired type I error rate. Here we show the same plots across all smoothness parameter values, and find largely the same results, showing the importance of c in the process for choosing null streets.

5.1 Global test results for negative control

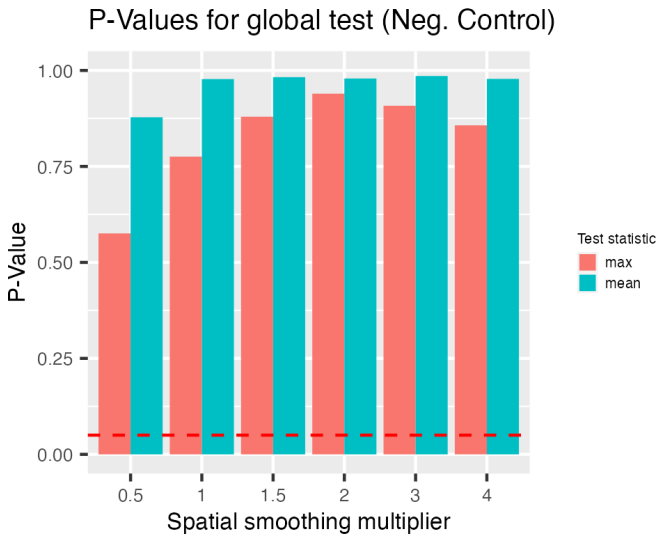

5.2 Histograms of the corrected p-values for various spatial smoothing levels

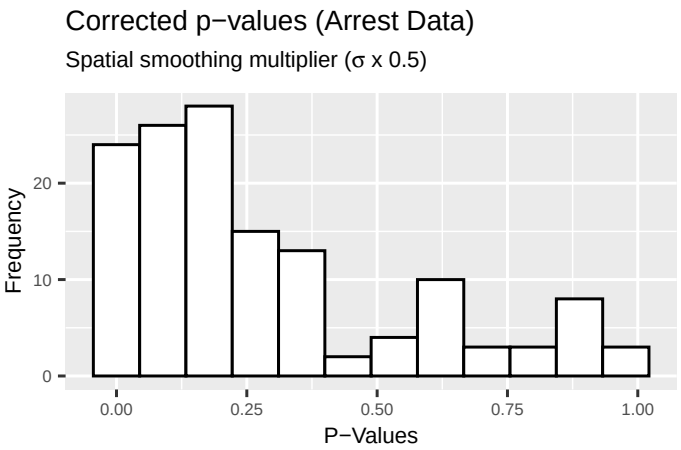

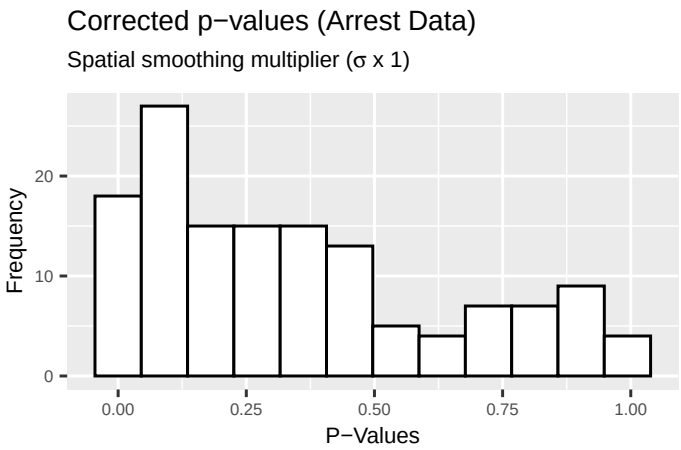

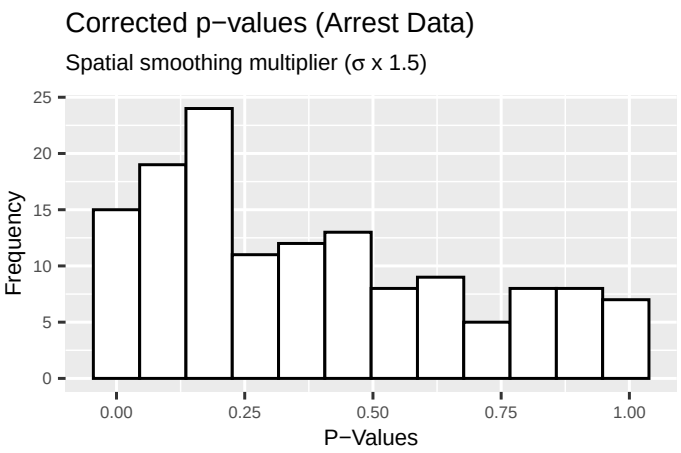

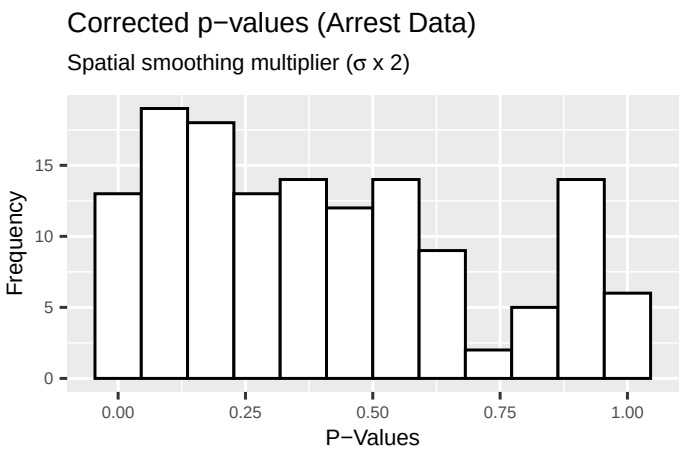

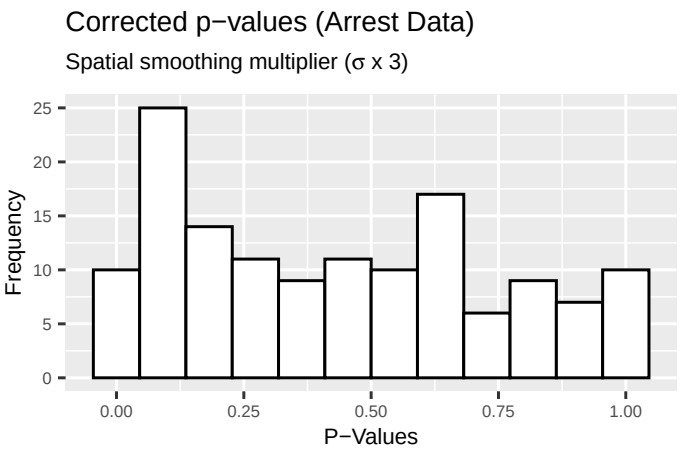

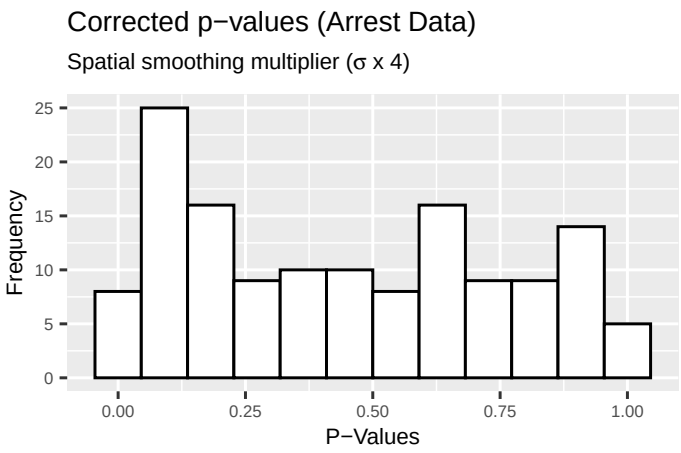

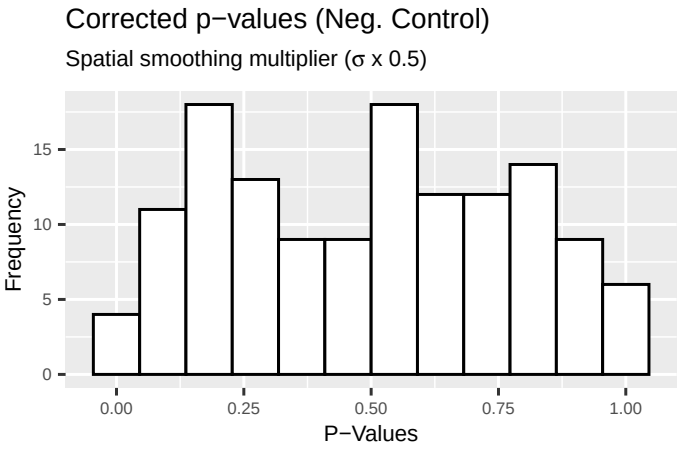
Corrected p−values (Neg. Control)
Spatial smoothing multiplier (σ x 0.5)
Frequency
P−Values
0
5
10
15
0.00
0.25
0.50
0.75
1.00

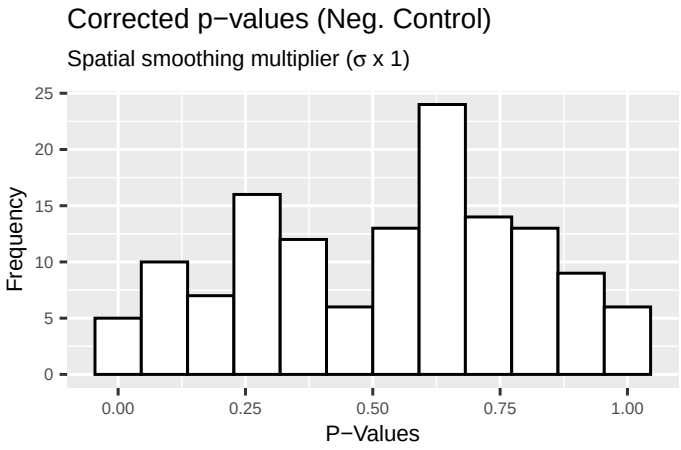
Corrected p−values (Neg. Control)
Spatial smoothing multiplier (σ x 1)
Frequency
P−Values
0
5
10
15
20
25
0.00
0.25
0.50
0.75
1.00

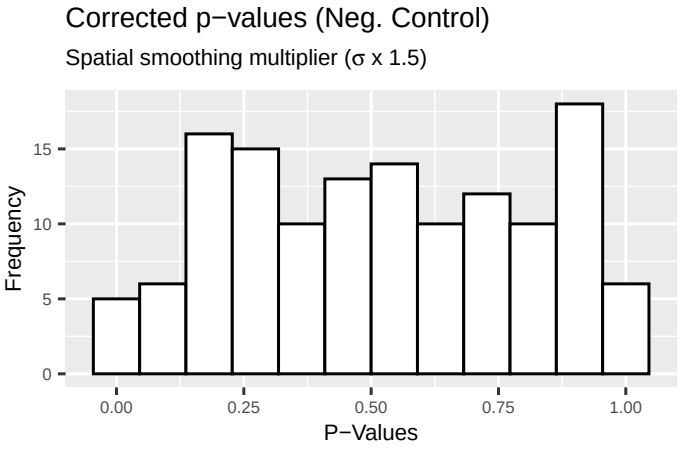
Corrected p−values (Neg. Control)
Spatial smoothing multiplier (σ x 1.5)
Frequency
P−Values
0
5
10
15
0.00
0.25
0.50
0.75
1.00

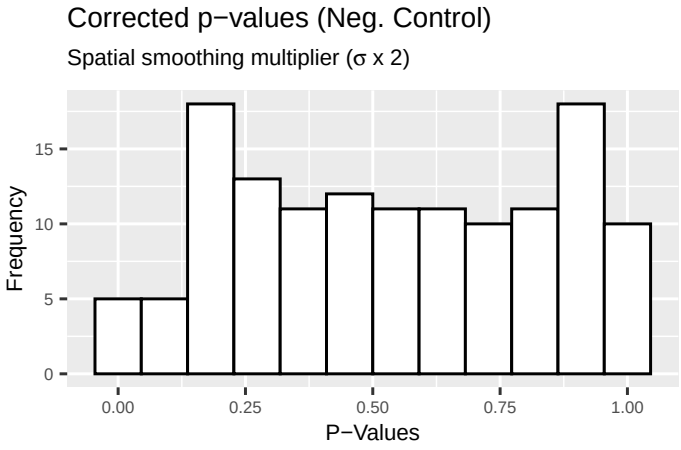
Corrected p−values (Neg. Control)
Spatial smoothing multiplier (σ x 2)
Frequency
P−Values
0
5
10
15
0.00
0.25
0.50
0.75
1.00

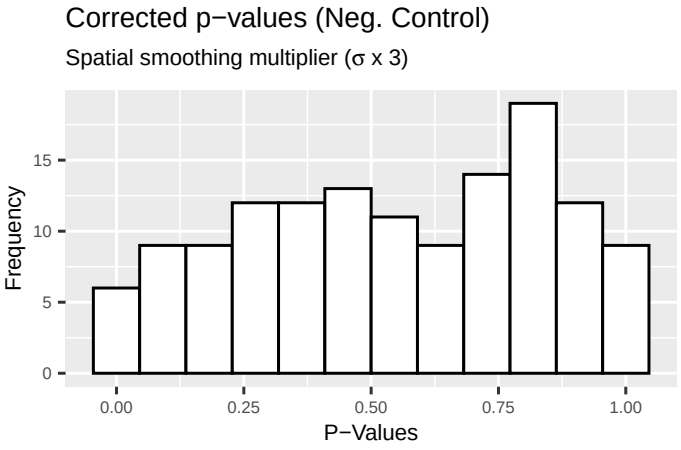
Corrected p−values (Neg. Control)
Spatial smoothing multiplier (σ x 3)
Frequency
P−Values
0
5
10
15
0.00
0.25
0.50
0.75
1.00

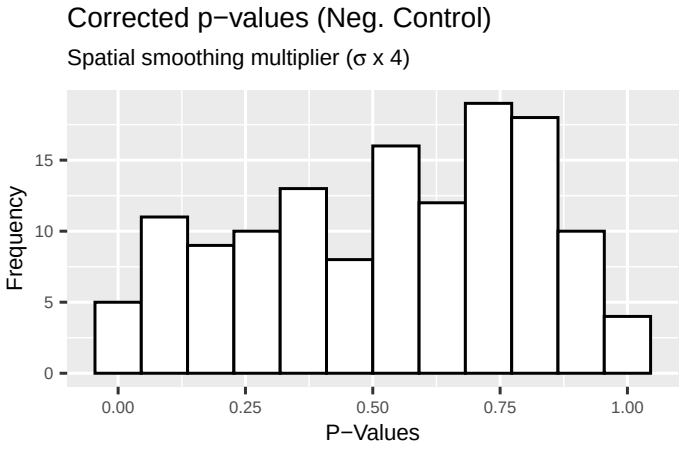
Corrected p−values (Neg. Control)
Spatial smoothing multiplier (σ x 4)
Frequency
P−Values
0
5
10
15
0.00
0.25
0.50
0.75
1.00

5.3 Type I error as a function of c

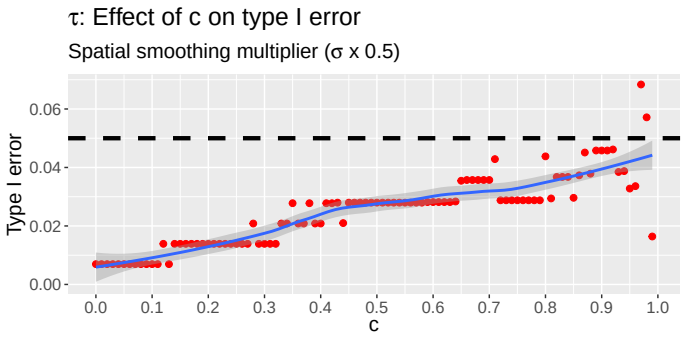

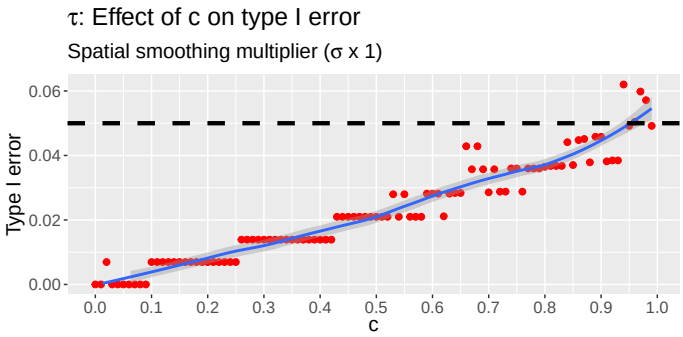

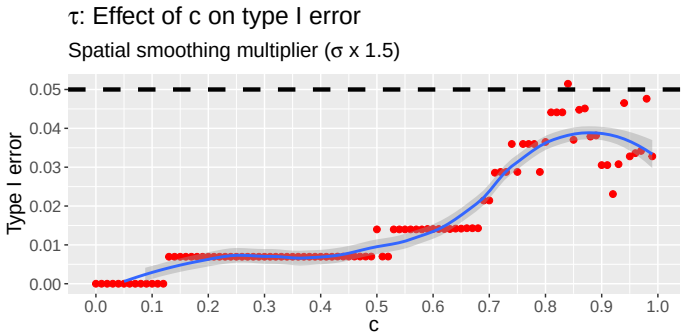

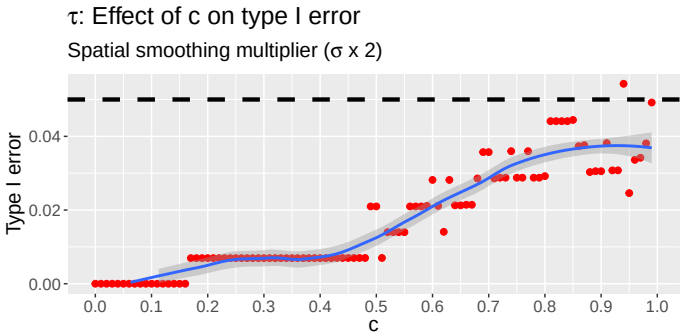

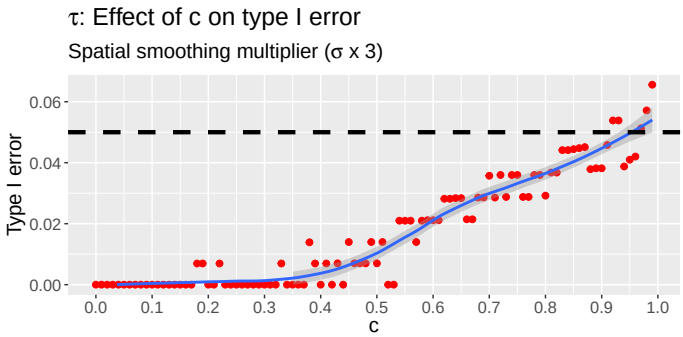

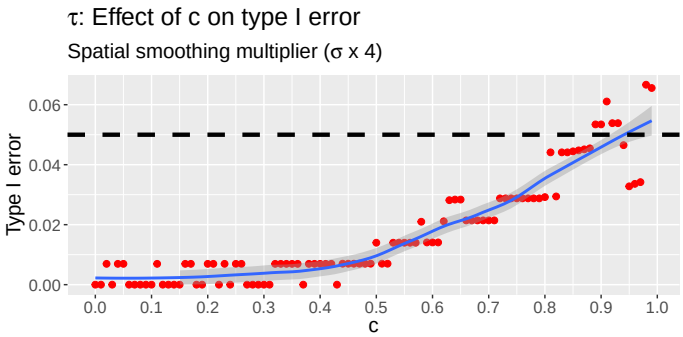

6 Results using $\theta(R_\delta)$ as estimand

Here we show the same results as in the manuscript, where instead we use $\theta(R_\delta)$ as the estimand instead of τ. We show results for both the arrest outcome as well as the negative control outcome for a variety of buffer widths, denoted by δ. Note throughout this section that our outcomes $Y(R^{(i)}_{\delta,0})$ and $Y(R^{(i)}_{\delta,1})$ are the counts of the number of events within a buffer width of δ around boundary i, divided by a scaling factor dependent on the outcome being examined. For arrests, we divide the total number of arrests by the amount of crime in a region to examine arrest rates instead of counts. For the negative control outcome, we scale the number of trees by the total length of streets in the region to obtain a rate of trees per length of street.

We first show the percentage of rejections across the 144 police precinct boundaries for both arrests and the negative control outcome. As expected, for the negative control outcome we see rejections in approximately 5% of the tests across all buffer widths, highlighting the utility of our proposed approach to inference. For the arrest data, we see similar results as for the τ estimand, though they are slightly more conservative. At small buffer widths, we see more than the 5% of rejections we would expect if there were no precinct effects, suggesting a small effect of precincts across the city. This effect dissipates, however, as the buffer width increases. We next show the results of the global test for both the mean and max as the global test statistic. For the negative control outcome, all of the p-values are well above 0.05 as expected given that this outcome should not be affected by police precincts. For the arrest data, at the smallest buffer width of 300 feet the p-values are smaller, yet still above the 0.05 threshold. These increase as the buffer width grows, which mirrors the results above for the individual tests showing some significant tests at a buffer width of 300 or 400 feet, which then disappear at larger buffer widths. We also show the p-value histograms, which mirror the results seen for τ. For the negative control outcome these are largely uniformly distributed, while for the arrest data they assign more weight to small p-values at lower buffer widths. Lastly, we investigate the choice of c on the type I error in the negative control outcome for $\theta(R_\delta)$. As for the τ estimand, the choice of c is very important for type I error control, though the value of c needed for valid type I error control is different for this estimand. For this estimand, small values of c also lead to conservative inference, but larger values of c lead to anti-conservative inference. The optimal choice of c depends slightly on the smoothing parameter, but a value of c around 0.65 leads to good type I error control in all analyses, which is therefore the value that we proceed with.

6.1 Proportion of p-values less than 0.05 using the corrected testing approach

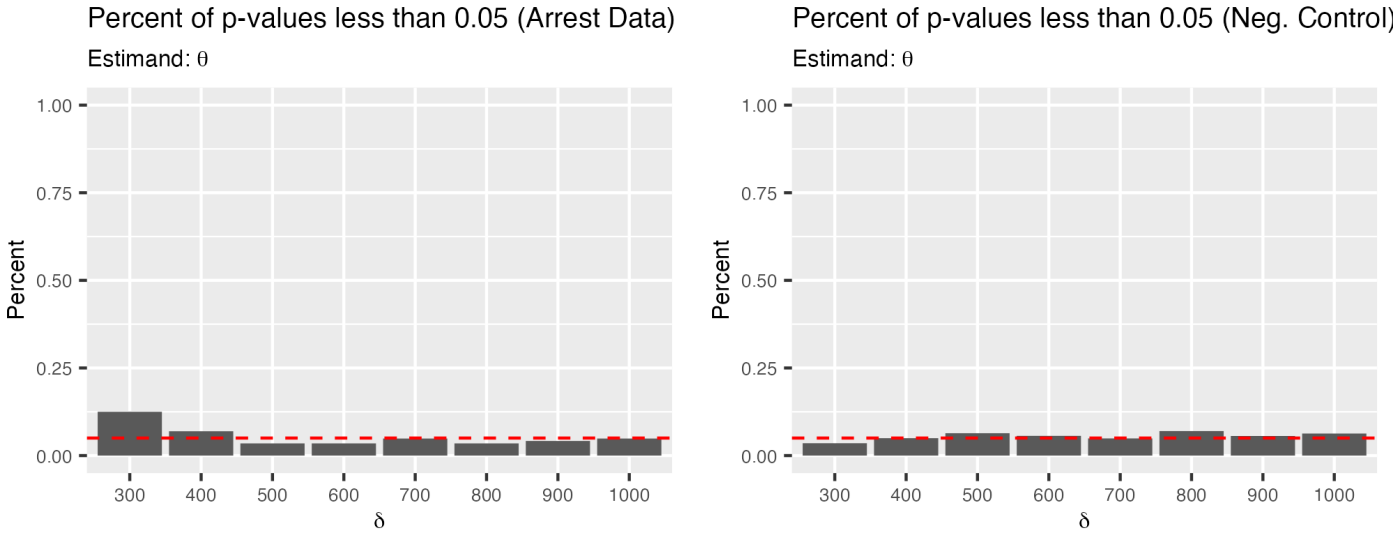

6.2 Global test results

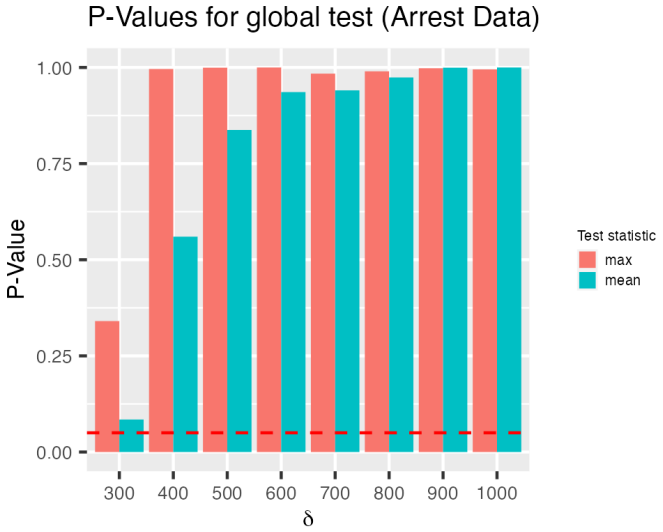

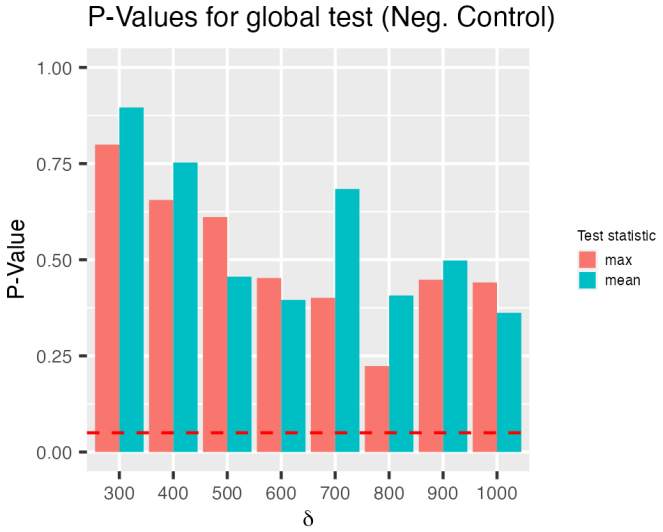

6.3 Histograms of the corrected p-values for various δ

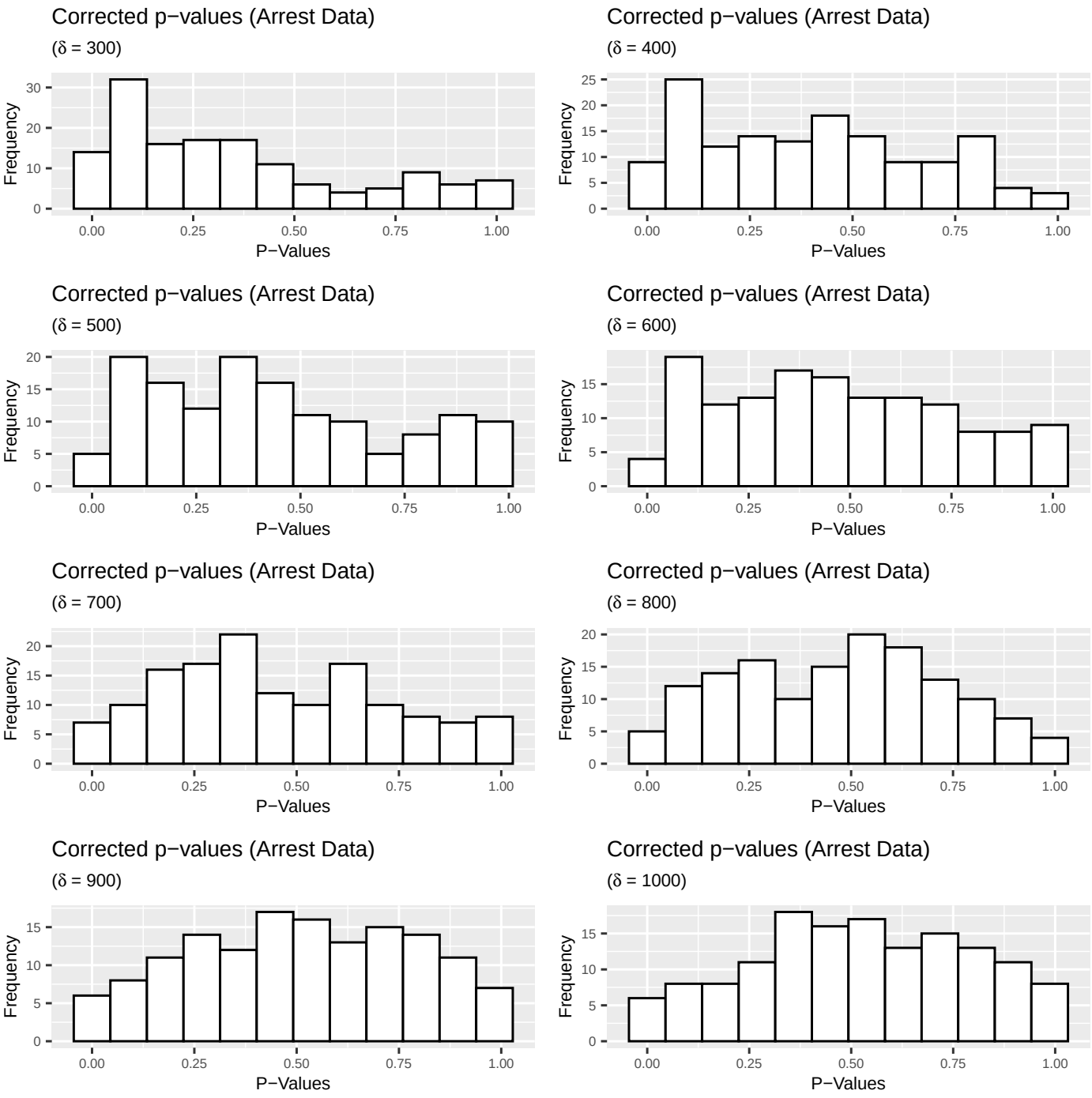

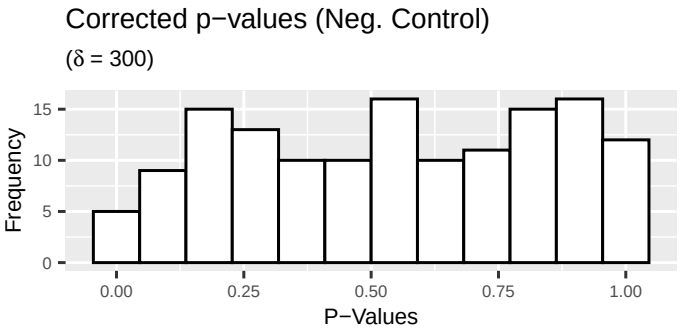
Corrected p−values (Neg. Control)
(δ = 300)
Frequency
P−Values

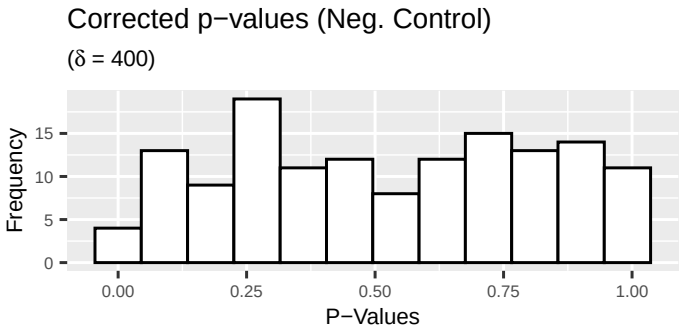
Corrected p−values (Neg. Control)
(δ = 400)
Frequency
P−Values

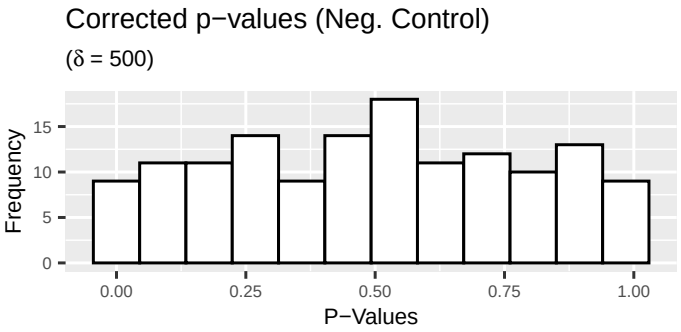
Corrected p−values (Neg. Control)
(δ = 500)
Frequency
P−Values

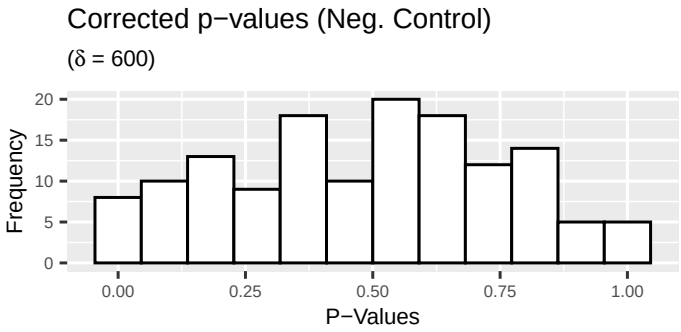
Corrected p−values (Neg. Control)
(δ = 600)
Frequency
P−Values

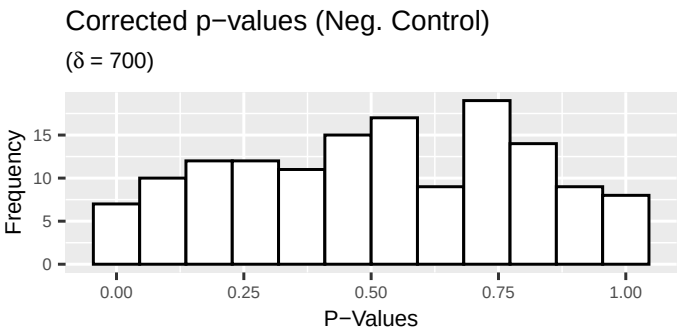
Corrected p−values (Neg. Control)
(δ = 700)
Frequency
P−Values

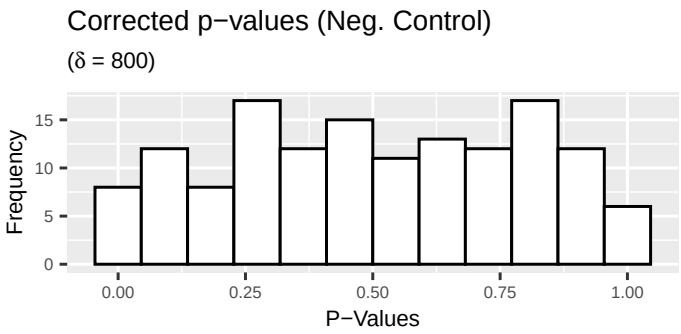
Corrected p−values (Neg. Control)
(δ = 800)
Frequency
P−Values

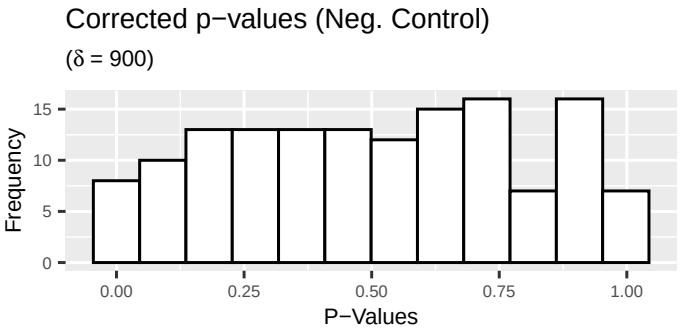
Corrected p−values (Neg. Control)
(δ = 900)
Frequency
P−Values

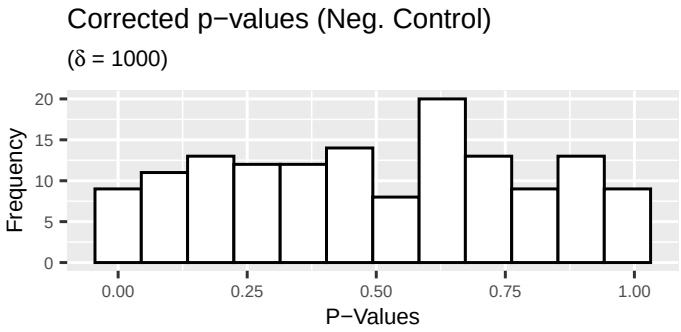
Corrected p−values (Neg. Control)
(δ = 1000)
Frequency
P−Values

6.4 Type I error as a function of c

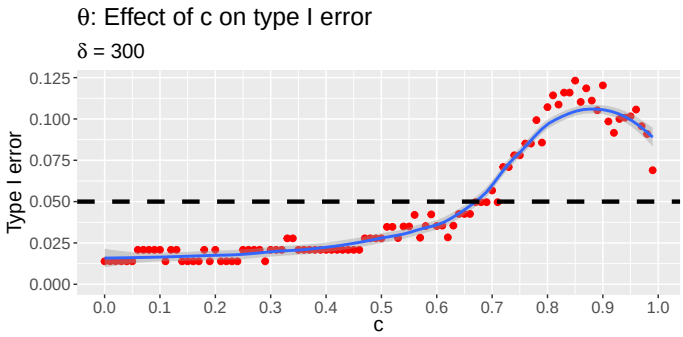

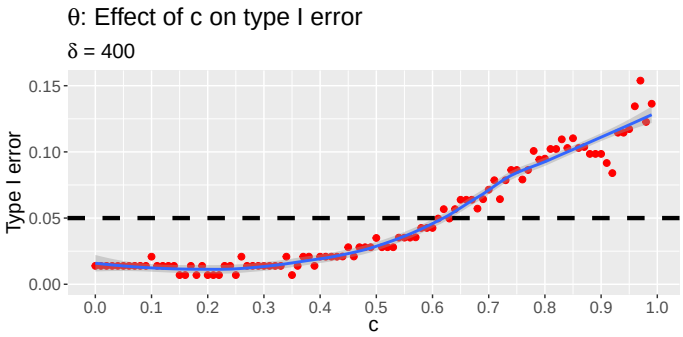

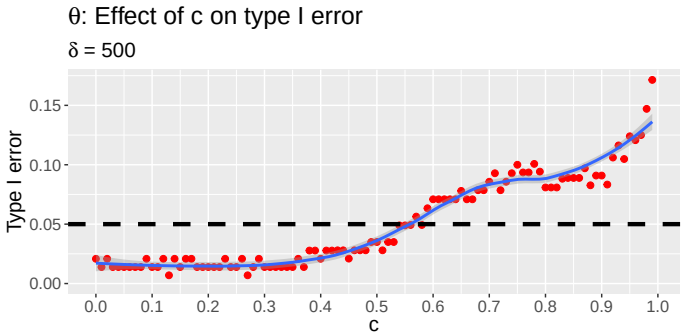

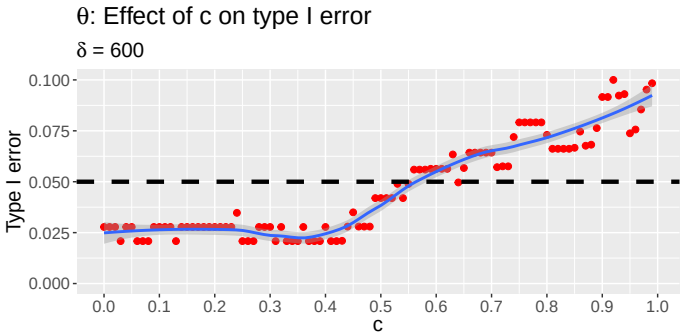

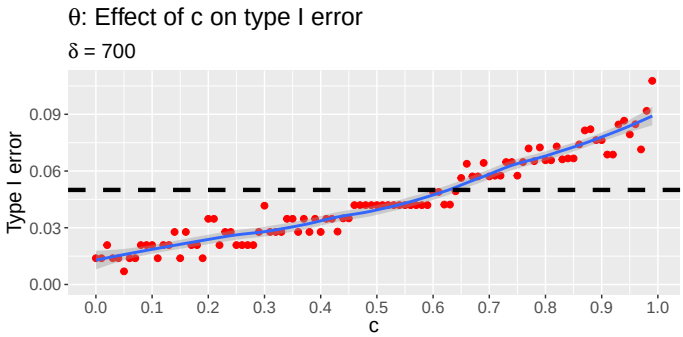

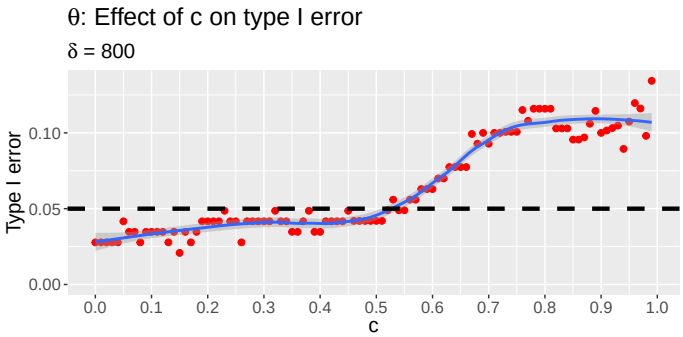

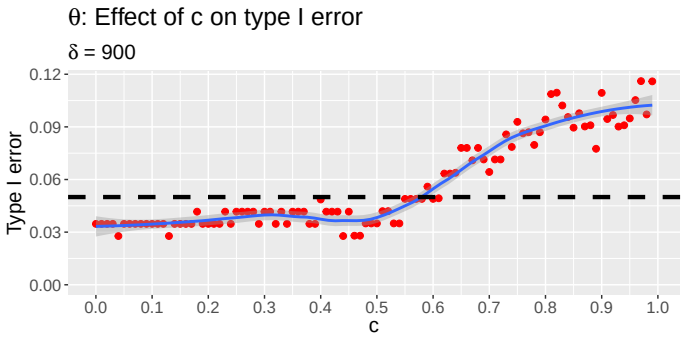

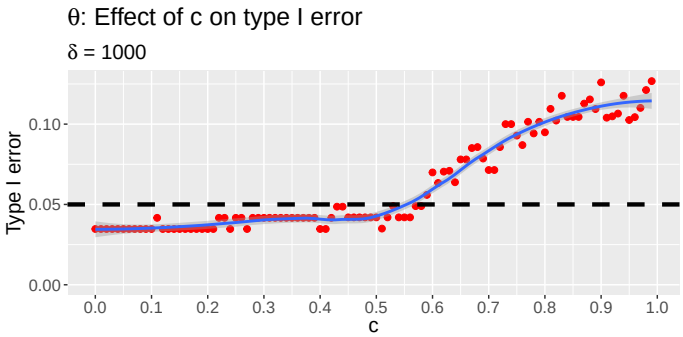

7 Map of all NYC precincts and streets

Here we show a map of all streets available in the NYC analysis. The red lines correspond to all streets in NYC that are available to be null streets, while the black lines correspond to precinct boundaries.